Hybrid simulations of the stellar wind interaction with close-in extrasolar planets

E. P. G. Johansson, T. Bagdonat, U. Motschmann
Institute for Theoretical Physics, Technical University of Braunschweig, Germany
(email: e.johansson@tu-bs.de)

Abstract

It is expected that the atmospheres of close-in extrasolar planets frequently undergo hydrodynamic expansion and produce strong ionospheres due to intensive photoionization, while at the same time being exposed to a strong stellar wind. This scenario can be expected to lead to new types of magnetospheres and interactions between stellar wind plasma and ionospheres previously unseen in the solar system. We have used a hybrid code, treating electrons as a massless, charge-neutralizing, adiabatic fluid and ions as macroparticles, to study the influence of a strongly expanding ionosphere on the stellar wind interaction for an unmagnetized close-in extrasolar terrestrial planet. We report on our attempts to apply this code to close-in extrasolar planets and results therefrom.

Introduction and motivation

Of the ~340 exoplanets discovered to date (exoplanet.eu), ~29% are within an orbital distance of a < 0.1 AU from their respective host stars. This opens up for the possibility of new types of planet-stellar wind interaction not seen in the solar system. One of these new scenarios is that of **stellar wind interaction with hydrodynamically expanding atmospheres**, a type of atmosphere in which the upper atmospheric layers are continuously expanding up to altitudes of ~planetary radii before being lost into space (Vidal-Madjar 2003, 2004; Lammer et al. 2004; Yelle 2004; Tian et al. 2005). This type of atmosphere has been suggested and theorized for ancient Venus, Mars as well as for Earth and is believed to be observed for close-in exoplanet HD 209458 b (e. g. Vidal-Madjar et al. 2003, 2004; Kasting et al. 1983; Lammer et al. 2008 and references therein).

Just as the *solar* wind interaction with several bodies in the solar system has long been studied, e. g. with hybrid codes (e. g. Boesswetter et al. 2007, Simon et al. 2007), our aim has been to use a hybrid code to start looking at the consequences of expanding atmospheres for the *stellar* wind interaction with close-in exoplanets (Johansson et al. 2009).

Simulation code

The basic simulation concept is an obstacle, i.e. an exoplanet with ionosphere, located in a three-dimensional simulation box which is then immersed in a moving stellar wind plasma and time integrated until reaching a quasistationary state. The ionosphere is modeled as a plasma producing region surrounding the planet. The hybrid code we have used was introduced in Bagdonat & Motschmann (2002).

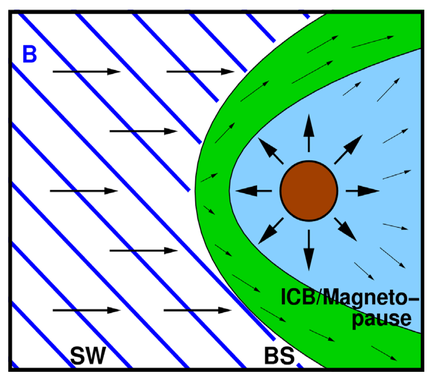

Hybrid model

- Plasma is modeled using a **hybrid model**, representing electrons as massless fluids (one per ion species s) and ions as (macro)particles.

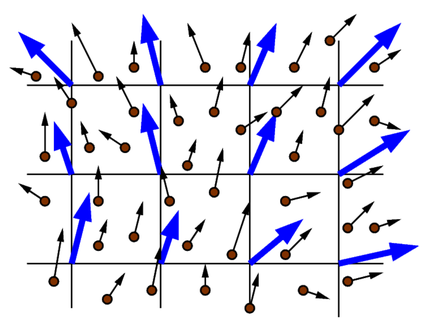

- The plasma is collisionless. The code does however permit the inclusion of drag forces due to a prescribed neutral background atmosphere as well as a prescribed finite plasma conductivity (neither is used in this work). This reduces the ion motion to

$$\frac{d\vec{v}_s}{dt} = \frac{q_s}{m_s}\left(\vec{E} + \vec{v}_s \times \vec{B}\right) - \frac{GM_\mathrm{p}}{r^2}\hat{r}$$

- The plasmas are quasineutral: $n_{\mathrm{i},s} = n_{\mathrm{e},s}$
- Electron pressure is assumed to be adiabatic:

$$p_{\mathrm{e},s} \propto \left(n_{\mathrm{e},s}\right)^{\kappa_s}$$

- The Darwin approximation of Ampere's law applies:

$$\nabla \times \vec{B} = \mu_0 \vec{j}$$

Numerics

Using the above assumptions one can express the state of the system with the help of the location and velocity of the macroparticles and the magnetic field alone. Using the particle time evolution equation above and the time evolution of the magnetic field which follows from above one can time integrate the system.

$$\frac{d\vec{B}}{dt} = \nabla \times \left(\vec{u}_\mathrm{i} \times \vec{B}\right) - \nabla \times \left(\frac{\left(\nabla \times \vec{B}\right) \times \vec{B}}{\rho_\mathrm{c}\mu_0}\right)$$

The time integration for the magnetic field is performed using a standard leapfrog technique using subcycling (smaller time steps) and the current advancement method (CAM) proposed by Matthews (1994).

A particle-in-cell (PiC) scheme is used to collect the moments of the distribution function from the macroparticles. These moments are then used to solve Maxwell's equations.

Stellar wind

Equivalent to solar orbit at ~0.1 AU, except the magnetic field strength which is artificially low due to computational constraints.

Number density	1 050 cm^{-3}
Magnetic field	6 nT
Velocity	300 km
Temperature	T_i = 250 000 K
	T_e = 500 000 K

Planet and ionosphere

We choose an Earth-sized, Earth mass planet and implement the ionosphere as a hydrogen plasma producing region surrounding the planet. The plasma is given an initial radial velocity since it originates from the ionization of an imagined *expanding neutral atmosphere* which is not part of our simulations. Due to the difficulties in actually modeling expanding neutral atmospheres together with resulting ionospheres, we instead use a simplistic postulated spherically symmetric ionosphere with production rate and initial radial velocity profiles according to figure 1. Atmospheric modeling has implied that these velocities would be of order 1-10 km/s at r~2 R_p (e. g. Yelle 2004, Tian et al. 2005) but observations hint that they can be up to ~100 km/s (Vidal-Madjar et al. 2003). We are interested in cases where the ionospheric expansion can compete with the stellar wind so we choose to investigate **three simulation scenarios** differentiated only by their initial ionospheric velocities, ranging from zero up to the extreme case of 100 km/s.

Total production rate	$2.46 \cdot 10^{30}$ s^{-1}
Initial temperature	T_i = 10 000 K
	T_e ~ 20 000 K
Initial radial velocity:	
a.) **Stationary scenario**	0 km/s
b.) **Expanding scenario**	~50 km/s
c.) **High-speed scenario**	~100 km/s

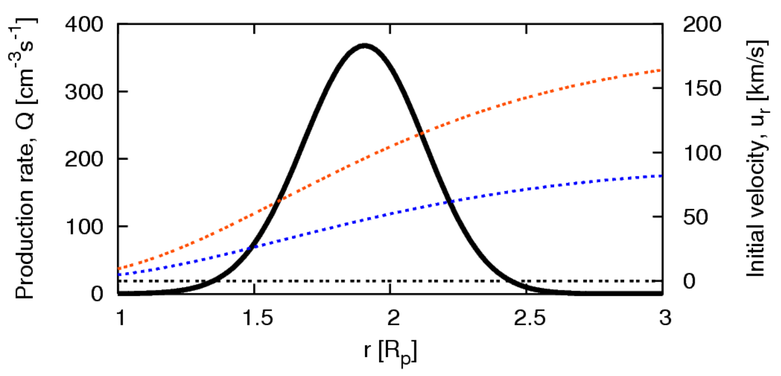

Figure 1: Ionospheric profiles used. Ionospheric production rate (solid black line), initial radial velocity for stationary ionosphere (dotted black), expanding ionosphere (dotted blue) and high-speed ionosphere (dotted red).

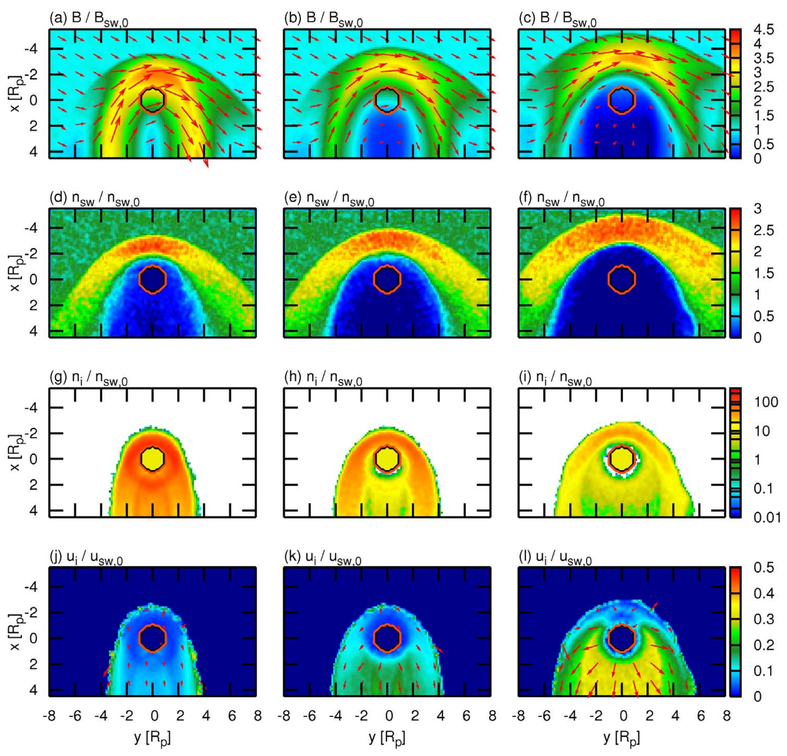

Figure 2: Comparison of simulation results for the three different ionospheric outflow scenarios, showing stationary atmosphere (left column), expanding atmosphere (middle column) and high speed atmosphere (right column), magnetic field (row 1), stellar wind density (row 2), ionospheric density (row 3) and ionospheric velocity (row 4). All subfigures are in the equatorial plane, here defined as the plane of the stellar wind velocity and magnetic field, $u_{\mathrm{SW},0}$ and $B_{\mathrm{SW},0}$. All values are normalized to the undisturbed stellar wind values. Stellar wind enters the simulation box from above.

Features

Comparing the three scenarios in figures 2 and 3 we can observe how “turning on” the expanding ionosphere influences the picture, i. e. by going from stationary to expanding to high-speed scenario:

- Increasing ionospheric dynamic pressure pushes the magnetopause and bow shock upstream and enlarges the effective obstacle.
- The magnetic draping is prevented from diffusing as far into the ionosphere as well as having to drape around the larger effective obstacle.
- A large undisturbed, low magnetic field region is created on the nightside. Proton gyration radii are here ~R_p but there are still no visible kinetic effects. (Is also true when looking at the polar plane which is not shown here.)
- Sharpening ion composition boundary (ICB) as the SW no longer reaches into and overlaps with the ionosphere (the ion producing region).
- Hints of instability on the ICB in the high speed scenario.
- Expansion speeds up the away transport of ionospheric plasma from the planet and the simulation box, leading to overall lower ionospheric densities.
- The initial expansion velocity given to the just created ionospheric ions is never translated into a upstream bulk flow around the subsolar point, but is instead immediately turned into thermal motion and thermal pressure.

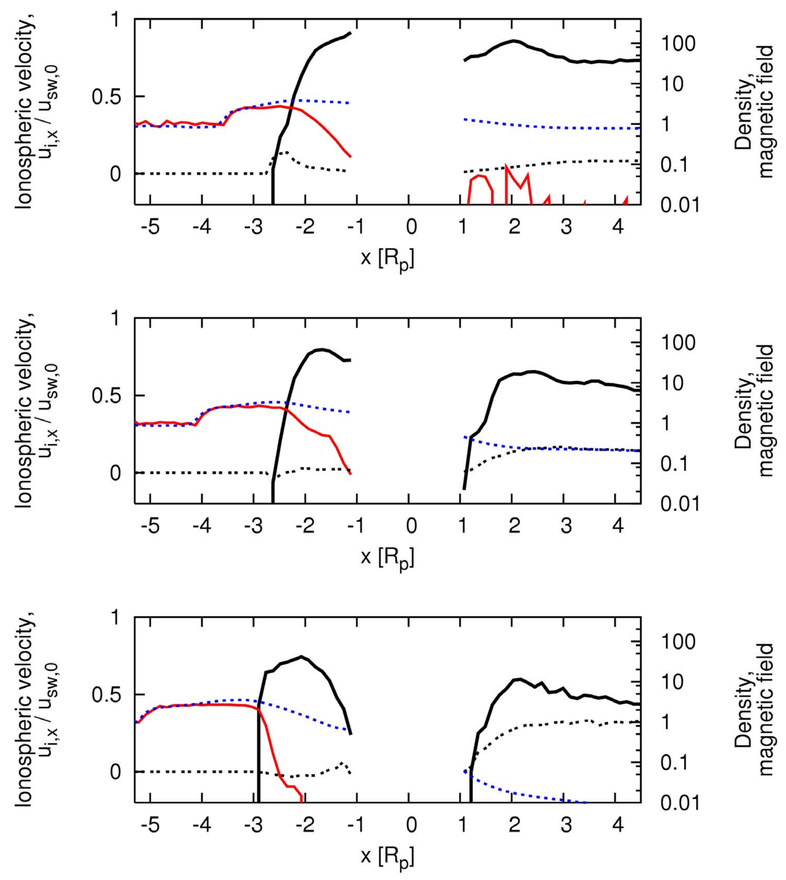

Figure 3: Stellar wind density (solid red line), ionospheric density (solid black), ionospheric x velocity (dotted black) and magnetic field y component (dotted blue) plotted as functions of position on the x axis for stationary (top), expanding (middle) and high-speed atmosphere (bottom). All values are normalized to the undisturbed stellar wind values. Notice that ionospheric velocity is on a linear scale while the other variables are on a logarithmic scale.

References

- Bagdonat, T. & Motschmann, U. 2002, Journal of Computational Physics, 183, 470
- Boesswetter, A., Simon, S., Bagdonat, T., et al. 2007, Annales Geophysicae, 25, 1851
- Johansson, E., Bagdonat, T., Motschmann, U., A&A, accepted
- Kasting, J. F. & Pollack, J. B. 1983, Icarus, 53, 479
- Lammer, H., Kasting, J. F., Chassefiere, E., et al. 2008, Space Science Reviews, 139, 399
- Lammer, H., Selsis, F., Ribas, I., et al. 2004, in ESA Special Publication, Vol. 538, Stellar Structure and Habitable Planet Finding, ed. F. Favata, S. Aigrain, & A. Wilson, 339–342
- Matthews, A. P. 1994, J. Comput. Phys., 112, 102
- Simon, S., Boesswetter, A., Bagdonat, T., Motschmann, U., & Schuele. 2007, Annales Geophysicae, 25, 117
- Tian, F., Toon, O. B., Pavlov, A. A., & De Sterck, H. 2005, ApJ, 621, 1049
- Vidal-Madjar, A., Desert, J.-M., Lecavelier des Etangs, A., et al. 2004, ApJ, 604, L69
- Vidal-Madjar, A., Lecavelier des Etangs, A., Desert, J.-M., et al. 2003, Nature, 422, 143
- Yelle, R. V. 2004, Icarus, 170, 167